Micelle-Bound Conformations of a Bombesin/Gastrin Releasing Peptide Receptor Agonist and an Antagonist by Two-Dimensional NMR and Restrained Molecular Dynamics

J. A. Malikayil,* J. Vincent Edwards, and Larry R. McLean

Marion Merrell Dow Research Institute, 2110 East Galbraith Road, Cincinnati, Ohio 45215

Received April 1, 1992; Revised Manuscript Received May 20, 1992

ABSTRACT: Two nonapeptide analogs of the carboxyl termini of bombesin (Bn) and gastrin releasing peptide (GRP) have been synthesized. Despite the small difference in chemical composition between these peptides, one was a potent agonist and the other a potent antagonist of the Bn/GRP receptor in murine pancreas. All protons of both peptides, in dodecylphosphocholine micelles, were assigned by two-dimensional nuclear magnetic resonance spectroscopy. Interproton distance were derived from cross-peak volumes in nuclear Overhauser enhancement spectra. Conformations of both peptides were derived by distance-restrained molecular dynamics simulations using the interproton distances as constrains. The agonist conformation resembled a relaxed helix formed by three connected turns. The two N-terminal turns were similar for both peptides. The third turn of the agonist, at the carboxyl terminus, was absent in the antagonist. One interproton distance at the carboxyl terminus of the antagonist indicates that the chemical group connecting the last two residues of this peptide mimics a cis peptide bond geometry.

Bombesin-like peptides are a family of amphibian skin peptides structurally related to the mammalian peptides gastrin releasing peptide (GRP)[1] and neuromedins (Erspamer, 1988). These peptides demonstrate high sequence homology at the carboxyl termini and possess a diversity of biological activities in numerous tissues and cell types. In the central nervous system of rat, bombesin causes hypothermia (Rivier & Brown, 1978), hyperglycemia (Brown et al., 1978), satiety (Negri, 1986), and grooming behavior. The identifying action of bombesin and GRP is stimulation of gastrin (McDonald, 1978). However, its mechanism of action in gastrin cells is not clearly understood. Bombesin stimulates secretion of pancreatic enzymes (Jensen et al., 1988) and effects the release of certain gastrointestinal hormones (Ghatei et al., 1982). It functions as a growth factor both in murine 3T3 cells and in small cell lung cancer cells (Cuttitta et al., 1985; Corps et al., 1985) and has been reported to stimulate natural killer cell activity (Van Tol et al., 1991). Recent work has identified bombesin and GRP activities in embryonic (Sunday et al., 1990) and pathological lung tissue (Aguayo et al., 1990).

It has been suggested that bombesin and GRP activate the same receptor (Bn/GRP receptor) and increase phosphatidylinositol turnover (Fanger et al., 1991). Cloning and functional characterization of Bn/GRP receptor (Spindel et al., 1990) suggest that this receptor belongs to the superfamily of G-protein-coupled receptors. Since the Bn/GRP receptor is one of a few neuropeptide receptors which has been cloned, it provides an important model for understanding ligand binding and activation in these systems. Previous studies have shown that bombesin analogs with small carboxyl-terminal modifications could yield receptor antagonists (Jensen & Coy, 1990). However, physicochemical studies probing the structural differences between agonists and antagonists have been scarce.

It has been shown that potent antagonists of bombesin may be derived through substitution of the penultimate amide bond with a CH_2NH group (Coy et al., 1988). On the basis of this result we synthesized peptide I and peptide II (Table I) differing only in the penultimate peptide bond position. Peptide I is a potent agonist while peptide II is potent antagonist of the Bn/GRP receptor in murine pancreas cells (Edwards et al., manuscript in preparation). Here we report the micelle-bound conformations of these two peptides as studied by 2D NMR and restrained molecular dynamics. These studies were conducted with the objective of delineating conformational differences between the two peptides that result in agonism and antagonism of the Bn/GRP receptor function.

EXPERIMENTAL PROCEDURES

Peptide Synthesis. Boc-Pheψ[CH_2S]Leu was prepared by the method of Spatola and Edwards (1986) and was attached directly to *p*-methylbenzhydrylamine resin with two DCC/HOBT couplings. For both peptides sequence elongation was accomplished by solid-phase methods on an Applied Biosystems Inc. 430A peptide synthesizer using double coupling of the preformed symmetrical anhydride or DCC/HOBT. Peptides were deblocked from the resin by HF cleavage. Purifications of the analogs were performed by reversed-phase HPLC, and the homogeneity of the preparations (98% or greater) was established by analytical reversed-phase HPLC. Amino acid analyses gave the expected results, and the integrity of the preparations was varified by FAB/MS.

Sample Preparation. H_2O samples of peptides for NMR studies were prepared by adding 700 μL of 50 mM sodium phosphate, pH 3.01 (95% H_2O/5% D_2O), to a mixture of the peptide and dodecylphosphocholine-d_{38} (DDPC, Merck Isotopes). Particulate matter in the preparation was removed by centrifugation. The clear solution was transferred into an NMR tube. The solution surface was thoroughly flushed with argon gas and was promptly sealed under a gentle flow of argon. The final pH of the sample in the NMR tube, in each

[1] Abbreviations: 2D, two dimensional; Bn, bombesin; CAMELSPIN, cross-relaxation appropriate for minimolecules emulated by locked spins; GRP, gastrin releasing peptide; NMR, nuclear magnetic resonance; TOCSY, total correlation spectroscopy; NOE, nuclear Overhauser effect; NOESY, 2D NOE spectroscopy; CD, circular dichroism, cmc, critical micelle concentration; DDPC, dodecylphosphocholine.

0006-2960/92/0431-7043$03.00/0

case, was 3.0. D_2O samples were prepared by an identical procedure with the exception that the buffer was prepared using 100% D_2O and the final pH meter reading was adjusted to 2.7 with dilute DCl. Peptide I concentrations for the H_2O and D_2O samples were respectively 3.9 and 2.9 mM. Peptide II concentrations were 13 mM for H_2O and D_2O samples. In all cases, the DDPC concentrations were 240 mM.

Measurement of Critical Micelle Concentration (cmc). The cmc of dodecylphosphocholine was determined from the concentration dependence of its surface tension in water. The surface tension of solutions at the air/water interface was measured by the du Nuoy ring method, in a specially constructed apparatus. A platinum–iridium ring of mean circumference $L = 6.000$ cm (No. 5020, Fisher Scientific Co., Pittsburgh, PA) was suspended from a linear variable differential transformer type force transducer (FTA-G10, Schevitz, Pennsauken, NJ) interfaced through a Data Translation (Marlborough, MA) DT-2801 A/D board to a 80286 class personal computer. Five measurements were averaged for each sample. The sample was then diluted, and measurements were continued until the solution surface tension approached that of the clean buffer. Surface tension of the sample (γ) was calculated from $\gamma = 2\Delta WLf$, where $\Delta W_{max} - W_{ring}$ and the correction factor $f = 0.7250 + (0.0004045 \times 2L + 0.014103)^{1/2}$ (Fisher Manual 15042), assuming a contact angle of zero and that the density of the sample equals that of water.

Circular Dichroic Spectra. CD spectra were recorded at room temperature on a JASCO J-500A spectropolarimeter using a 0.1-mm cuvette. Peptide spectra were collected in the same buffer that was used for the NMR studies. A spectrum for peptide II was also collected in 50 mM sodium phosphate, pH 5.9. The peptide and DDPC concentrations were respectively 2.6 and 250 mM for peptide I and 1.7 and 62 mM for peptide II. Data were collected at 0.04-nm intervals and were averaged over a 0.2-nm interval. The scan rate was 2 nm/min and the time constant was 8 s. The spectrum of air was subtracted after each scan.

NMR Spectroscopy. All NMR spectra were acquired on a Varian Unity 500 spectrometer equipped with a Sun 4/110 computer and a digital-phase shifter. All spectra were acquired at 25 °C in the phase-sensitive mode by the hypercomplex method of States et al. (1982). Time domain data were transferred to an Silicon Graphics 4D/35 computer to be processed by Felix (Hare Research, Seattle, WA).

Total correlation spectra (TOCSY) were collected with a mixing time of 60 ms (Davis & Bax, 1985). An MLEV-16 composite pulse was used for spin locking. A 2-ms trim pulse was applied at the end of the spin-lock pulse. A total of 400 t_1 data points were collected. NOESY spectra were acquired with mixing intervals of 25, 50, 100, and 150 ms. In this case 450 time increments were acquired. 2D CAMELSPIN spectra (Bothner-By et al., 1984) were acquired with a spin-locking field strength of 5 kHz and a spin-locking period of 250 ms. Small flip angle pulses (30°) were employed for spin-locking to reduce Hartmann–Hahn transfers (Kessler et al., 1987).

TOCSY and CAMELSPIN spectra were zero filled to final matrix sizes of 1K × 1K real points. A skewed sine bell was applied on both dimensions prior to Fourier transform. In the case of NOESY spectra, a squared cosine bell was applied along both dimensions, and matrices were zero filled to final sizes of 2K × 2K real points. No baseline correction was performed in any spectra. Instead, the first data point was zeroed and was calculated by a linear prediction routine (Marion & Bax, 1989). Since this procedure allowed for a model-free extrapolation of the first data point from correctly sampled data, cross-peak volumes of different data sets could be compared without the errors associated with polynomial fitting procedures. In most cases this procedure along F_1 alone yielded good quality spectra. Where necessary the procedure was also followed in the F_2 dimension.

Interproton Distances. Interproton distances were derived from cross-peak volumes in 50-ms NOESY spectra by the two-spin approximation assuming identical spectral density functions for all protons. In peptide I the distance between the geminal protons of glycine was used as reference. In peptide II geminal protons of glycine had degenerate chemical shifts. Therefore, the interproton distance of the $\psi[CH_2S]$ group was used as the reference distance in peptide II. In both instances the reference distance was taken as 1.79 Å. An upper-bound distance of 5.0 Å was assigned to cross-peaks that were only observed in D_2O and at the high mixing time of 200 ms. For both peptides the 2H, 6H and 3H, 5H protons of phenylalanine side chains were not resolved from the 4H proton. Therefore, two pseudoatoms were defined for the phenylalanine sidechain, (1) the arithmetic mean of 2H, 6H and 4H and (2) the arithmetic mean of 3H, 5H and 4H. The NOE constraints involving these pseudoatoms were relaxed by 2.4 Å. Pseudoatoms were also defined for side-chain methylene protons since stereospecific assignments were not achieved. In these instances the NOE constraints were relaxed by 1.0 Å.

Computational Procedures. Restrained molecular dynamics and restrained energy minimizations were performed on a Silicon Graphics 4D/35 computer using the DISCOVER molecular mechanics software with consistent valence force field (Biosym Technologies, Inc.). Calculations were carried out in vacuo. The initial structure was hand built as an extended strand using standard. Nonbonded pair interactions were reduced to zero at a cutoff distance of 8.0 Å. The system was coupled to a heat bath with a temperature coupling constant of 200 fs. The integration time step was 1 fs. Molecular geometries were stored at 1-ps intervals.

The distance restraint was applied as a skewed biharmonic potential (E_{NOE}) added to the total energy of the system

$$\begin{aligned} E_{NOE} &= c_1(r_{ij}^{0} - r_{ij}^{u})^2 \quad \text{for } r_{ij}^{u} < r_{ij}^{0} \\ &= 0 \quad \text{for } r_{ij}^{l} < r_{ij}^{0} < r_{ij}^{u} \\ &= c_2(r_{ij}^{0} - r_{ij}^{l})^2 \quad \text{for } r_{ij}^{l} > r_{ij}^{0} \end{aligned}$$

where r_{ij}^{0}, r_{ij}^{u}, and r_{ij}^{l} were respectively calculated, upper-bound target, and lower-bound target distances. The force constants c_1 and c_2 were given by $c_1 = 0.5kTS(\Delta_{ij}^{+})^{-2}$ and $c_2 = 0.5kTS(\Delta_{ij}^{-})^{-2}$, where k is the Boltzmann constant, T is the absolute temperature, S is a NOE-scale factor, and Δ_{ij}^{+} and Δ_{ij}^{-}, respectively, were error estimates on the upper-bound and lower-bound distances.

The same procedure was applied for the refinement of both structures. Initially 10 ps of restrained molecular dynamics, with an NOE-scale factor of 0.1, was conducted at 600 K using NOE-derived distances involving backbone protons as the only constraints. Distances involving pseudoatoms were not included during this stage. Following this step another 10 ps of dynamics was conducted at 300 K, with an NOE-scale factor of 0.2, including all available NOE-derived distances. The NOE-scale factor was then raised to 0.5, and 200 ps of distance-restrained dynamics simulation was carried out under these conditions. Molecular trajectories were stored only during the last stage of the simulation.

Table I: Amino Acid Sequences of the Peptides

porcine gastrin releasing peptide (GRP)	Ala-Pro-Val-Ser-Val-Gly-Gly-Gly-Thr-Val-Leu-Ala-Lys-Met-Tyr-Pro-Arg-Gly-Asn-His-Trp-Ala-Val-Gly-His-Leu-Met-NH_2
bombesin	Glp[a]-Gln-Arg-Leu-Gly-Asn-Gln-Trp-Ala-Val-Gly-His-Leu-Met-NH_2
peptide I	Glp[a]-Gln-Trp-Ala-Val-Gly-His-Phe-Leu-NH_2
peptide II	Glp[a]-Gln-Trp-Ala-Val-Gly-His-Pheψ[CH_2S]Leu-NH_2

[a] Glp = pyroglutamic acid.

RESULTS AND DISCUSSION

The primary structures of GRP, bombesin, peptide I, and peptide II are presented in Table I. The four peptides show a high degree of sequence homology in the carboxyl-terminal nonapeptide region. Peptide I and peptide II differ only in the nature of the chemical group that connects Phe^8 and Leu^9, which is a peptide bond in the former case and a ψ[CH_2S] group in the latter. Despite this small difference in chemical structure, the former peptide is a potent agonist (K_d = 0.2 nM) and the latter a potent antagonist (K_d = 3 nM) of GRP-induced phosphoinositol turnover of the Bn/GRP receptor in murine pancreas (Edwards et al., manuscript in preparation). Thus a comparison of the conformations of these peptides should prove useful for the design of substances that modulate the function of the Bn/GRP receptor.

In membrane environments bombesin-like peptides are suggested to adopt secondary structures that possibly resemble the receptor triggering conformation (Erne & Schwyzer, 1987). Therefore, we studied the conformation of peptide I and peptide II in dodecylphosphocholine micelles. Micelles were prepared by dissolving dodecylphosphocholine in phosphate buffer. The cmc for this system was 1 mM. The strong negative NOEs, even among side chains, and the ability to detect all sequential $d_{\alpha N}$ and d_{NN} NOEs show that both peptides assume a relatively rigid backbone conformation in the micellar environment. Absence of chemical shift multiplicities indicates a single predominant conformation with conformational averaging, if any, occurring at rates faster than the time scales of proton chemical shifts. 2D CAMELSPIN spectra did not contain any cross-peaks that were not observed in NOESY spectra.

The structural calculations reported in this study were based on NMR data collected at pH 3.0. Except for the chemical shift differences of amide proton resonances, the NOE patterns and TOCSY spectra of both peptides were essentially the same at pH 3.0 and 6.0. CD spectra of peptide II at pH 3.0 and 6.0, shown in Figure 1, were also similar. Therefore, the structures at pH 3.0 should be valid for pH values in this range.

All protons of both peptides were assigned by the sequential assignment procedure. For peptide II assignments proceeded smoothly since resonance overlap did not pose a problem. However, the resonances of His^7 and Phe^8 were in complete overlap in peptide I at pH 3.0. These resonances were unambigously assigned using spectra at pH 6.0 based on the amide resonance shift to varying pH. The sequential assignments are followed by constructs drawn in the NH–C_αH and NH–NH regions of 50-ms NOESY spectra for both peptides in Figures 2 and 3. Because of the large line widths homonuclear coupling constants were not measurable in the micelle-bound states of the peptides. Therefore, stereospecific assignments were not possible for methylene protons. Full resonance assignments for both peptides are shown in Table II.

Distance-restrained molecular dynamics simulations were used to derive conformations consistent with the NMR distances. Peptide II yielded a good quality NOESY spectrum

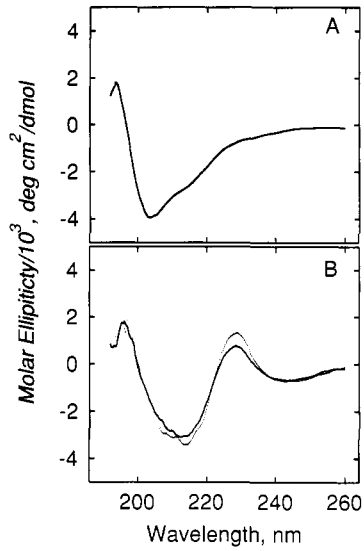

FIGURE 1: CD spectra of peptide I (A) and peptide II (B). In panel B, the solid spectrum was recorded at pH 3 and the broken-line spectrum was recorded at pH 6.

in H_2O at 25-ms mixing time. However, the spectral quality of peptide I at this mixing time was low due to the lower peptide concentration in this sample. The NOE-buildup pattern, in both peptides, did not show any evidence of spin diffusion at 50-ms mixing time. Therefore, interproton distances for both peptides were derived from cross-peak volumes in 50-ms NOESY spectra by the two-spin approximation assuming identical spectral density functions for all protons. The full lists of NOE-derived distances for both peptides are presented as supplementary material. Since the above assumptions used in distance derivations could be restrictive for peptides of this size, special care was taken in applying moderate NOE-forcing potentials. On the basis of the confidence warranted by the NOESY data, NOE-forcing potentials were adjusted by a scale factor and by the error margins placed on the upper-bound distance. For example, the error margin on the upper-bound distance was 0.1 Å for a distance involving a well-resolved backbone-backbone NOE. For such a distance involving a backbone–side-chain NOE and a side-chain–side-chain NOE, the error margins used were 0.3 and 0.4 Å, respectively. The NOE-scale factor (Δ_{ij}^+) and thereby the corresponding force constant (c_1) for NOEs involving side chains were deliberately maintained low since the NOE intensities in these cases are prone to dynamic errors. For peptide I, 33 interresidue and 21 intraresidue NOEs were identified. For peptide II there were 58 interresidue and 34 intraresidue NOEs. The lower number of observed cross-peaks on peptide I is due to the lower peptide concentration in this sample. The NOE-forcing potentials were introduced gradually in three steps as discussed under Experimental Procedures. This procedure allowed the distance constraints to be applied without the introduction of cis peptide bonds. The absence of cis peptide bonds in either peptide was evident by the absence of NOEs characteristic of this bonding geometry (Wuthrich, 1986).

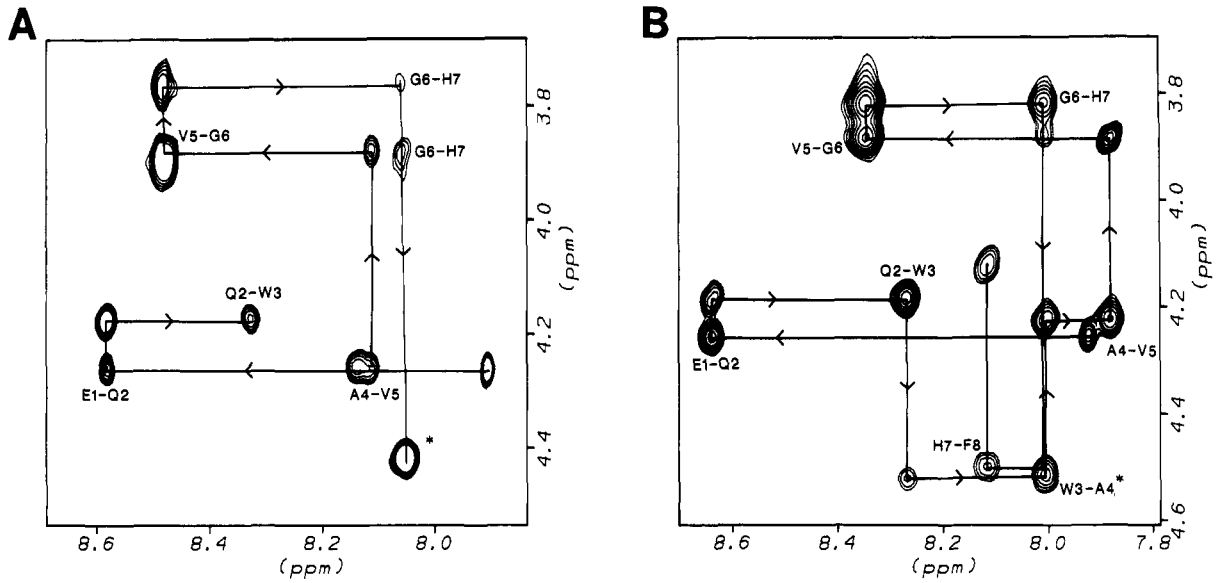

FIGURE 2: Fingerprint region of the 50-ms NOESY spectra of peptide I (A) and peptide II (B). The constructs follow the sequential connectivities.

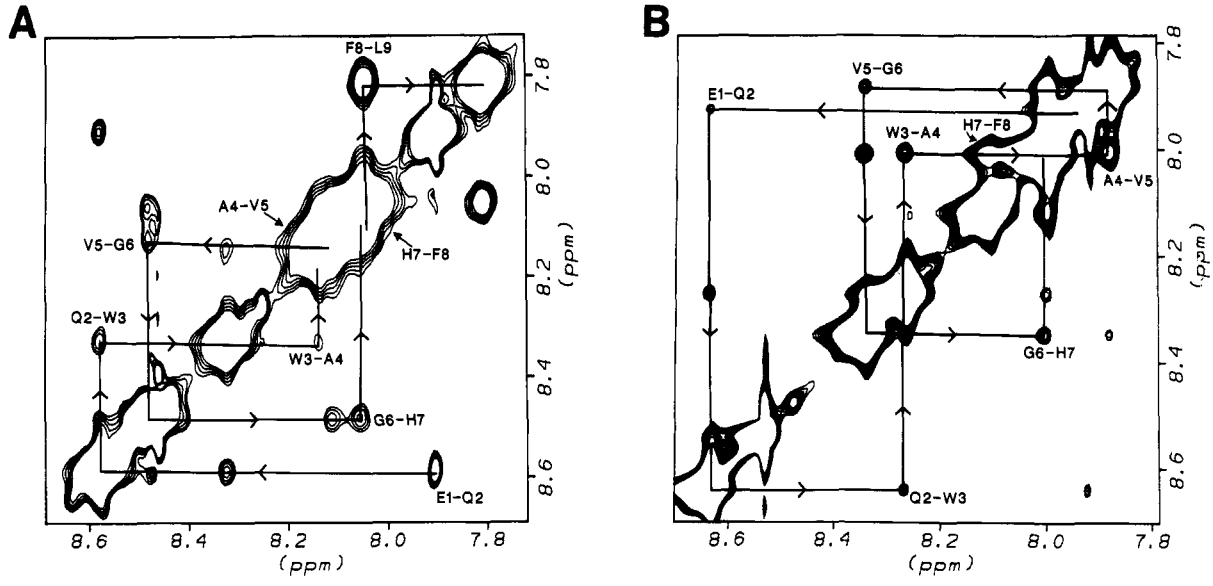

FIGURE 3: NH–NH region of the 50-ms NOESY spectra of peptide I (A) and peptide II (B). The constructs follow the sequential connectivities.

During the last 100 ps of simulation stable molecular dynamics trajectories were observed for both peptides. The variations in molecular geometries during this period were fluctuations about a predominant average conformation. A superposition of conformations at the end of every 5 ps of dynamics during the last 100 ps is shown in Figure 4. This figure shows that both peptides demonstrated conformational rigidity during simulation. The amino-terminal residue was relatively flexible in both peptides.

Figure 5 shows the average backbone conformation of each peptide during the last 64 ps of molecular dynamics. These conformations were calculated by converting the time domain data of the dynamics trajectory to the frequency domain and back-transformation to the time domain with filtering of all motional frequencies. Thus these molecular geometries represent the positional averages of the atomic coordinates during the last 64 ps of the simulation. The lack of distortions in bond lengths and bond angles in these conformations reflects the relative conformational rigidities of the peptides during the respective simulation periods. The dihedral angles of these average conformations are presented in Table III. The backbone proton–proton distances of the average structures are presented with the corresponding NOE-derived distances in Table IV. Overall, the correspondence between the experimental and calculated distances is very good.

The conformation of peptide I in the Gln^2–Leu^9 region could be best described as a relaxed helix formed by the linear arrangement of three connected β-turns. These three turns are comprised of residues Gln^2–Val^5, Ala^4–His^7, and Gly^6–Leu^9, respectively. A similar conformation is also observed for peptide II in the region Gln^2–His^7. However, the carboxyl-terminal turn of the previous structure is disrupted in peptide II due to the introduction of the ψ[CH$_2$S] group between Phe^8 and Leu^9. Thus the absence of the third turn at the carboxyl terminus is the difference in backbone conformations between peptide I and peptide II.

Both NMR-derived structures described above or even a qualitative interpretation of the $d_{\alpha N}$ and d_{NN} NOE patterns and the proton chemical shifts suggests that the backbone conformations of the two peptides are largely similar for the first seven residues. The CD spectra of the two peptides are

Table II: Chemical Shifts (in ppm)[a]

residue	NH	$C_\alpha H$	$C_\beta H$	other
peptide I				
Glp[1]	7.92	4.28	2.37, 2.27	1.76 ($C_\gamma H$)
Gln[2]	8.58	4.20	2.01, 1.97	2.31 (γCH_2)
Trp[3]	8.33	4.61	3.32, 3.25	10.57 (HE1), 7.33 (HD1), 7.47 (HE3), 6.97 (HZ3), 7.06 (HH2), 7.41 (HZ2)
Ala[4]	8.15	4.28	1.24	
Val[5]	8.12	3.90	2.08	0.97 ($C_\gamma H$)
Gly[6]	8.49		3.89, 3.76	
His[7]	8.06	4.46	3.15, 3.03	8.48 (HE1), 6.77 (HD2)
Phe[8]	8.05	4.26	3.15, 3.03	3.30 (HD1, HD2), 7.15 (HE1, HE2)
Leu[9]	7.81	4.26	1.66, 1.59	1.63 (γCH), 0.87 (δCH_3), 7.11, 7.02 (δNH_2)
peptide II				
Glp[1]	7.92	4.27	2.33, 2.25	
Gln[2]	8.63	4.21	2.02, 1.97	2.33 (γCH_2)
Trp[3]	8.26	4.53	3.32, 3.25	10.57 (HE1), 7.35 (HD1), 7.45 (HE3), 6.95 (HZ3), 7.03 (HH2), 7.41 (HZ2)
Ala[4]	7.99	4.23	1.15	
Val[5]	7.87	3.89	2.08	0.92 (γCH_3)
Gly[6]	8.34	3.86		
His[7]	8.01	4.52	3.07, 2.89	8.54 (2H), 7.04 (4H), 7.23 (2H, 6H), 7.14 (3H, 5H)
Phe[8]	8.11	4.14	3.09, 2.82	7.23 (2H, 6H), 7.14 (3H, 5H)
Leu[9]		3.44	1.71, 1.40	1.73 (γCH), 0.90 (δCH_3), 7.62, 7.08 (δNH_2)

[a] Chemical shifts are referenced to the residual HDO line set at 4.8 ppm. Glp = pyroglutamic acid.

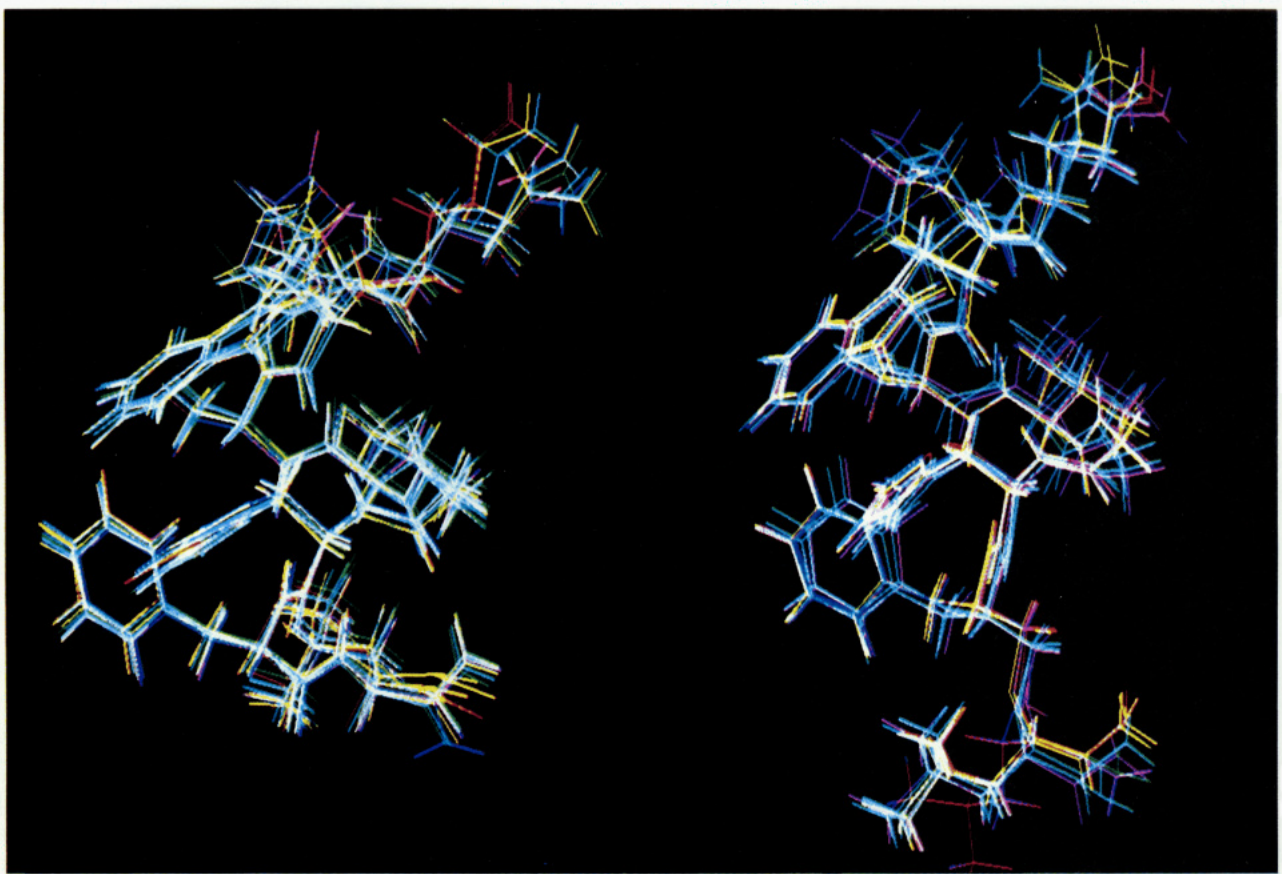

FIGURE 4: Superposition of the molecular conformations at the end of every 5 ps during the restrained molecular simulation. Peptide I (left) and peptide II (right).

significantly different in the range of 220–260 nm (see Figure 1) despite the high degree of similarity between the backbone conformations. This difference cannot be attributed to CD absorption of the $\psi[CH_2S]$ moiety since the dipeptide Pheψ-$[CH_2S]$Leu-NH_2 showed no CD absorption in this region (spectra not presented). Differences below 220 nm could be due to the presence of the $\psi[CH_2S]$ group in peptide II since the pseudodipeptide showed a weak negative band in this region. The 220–260-nm region of the spectrum contains peptide bond transitions and transitions that can be attributed to aromatic side chains (Brahms & Brahms, 1980). On the basis of the NMR-derived structures we attribute the most significant difference in the CD spectra, the positive band around 230 nm in peptide II, to differences in the orientations of the aromatic side chains in the two peptides. The available NMR data are not sufficient to determine the χ_2-dependent orientations of side chains. However, the different orientations of the aromatic side chains in the two peptides are apparent in the NOESY spectra. In peptide II, NOEs are detected among all three aromatic rings whereas in peptide I ring–ring NOEs are absent between Trp and His. However, the proximity of these two residues in peptide I is indicated by

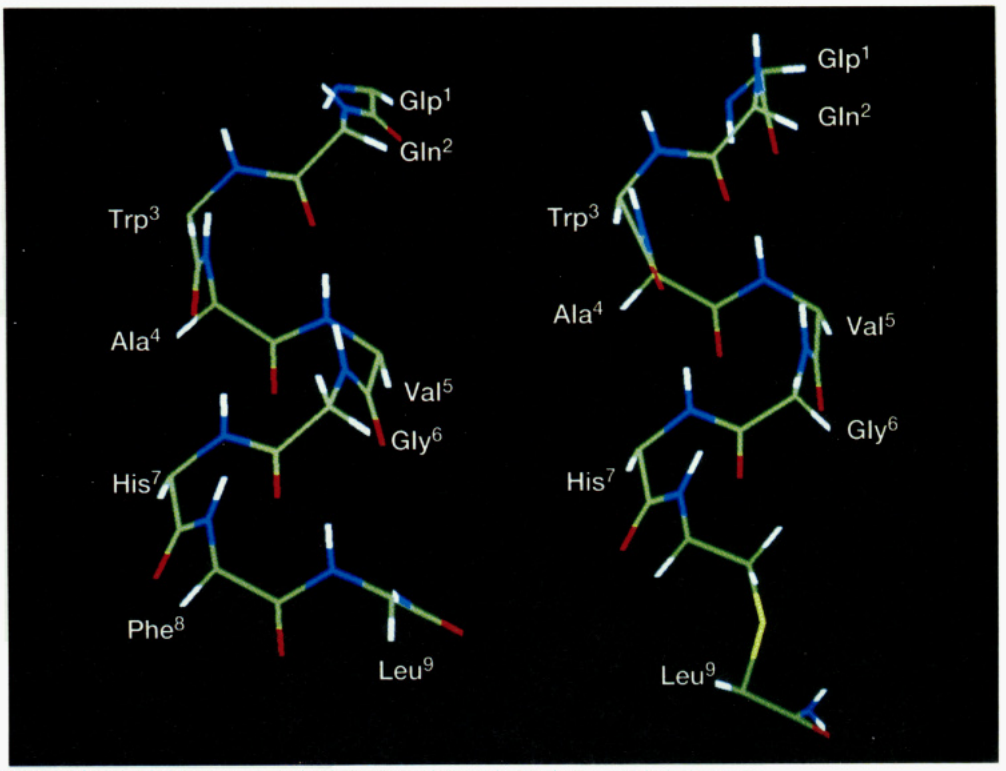

FIGURE 5: Positional-average backbone conformations of peptide I (left) and peptide II (right).

Table III: Dihedral Angles of Peptide I and Peptide II[a]

residue	ϕ	ψ	ω	χ_1
peptide I				
Glp[1]		−50	−180	56
Gln[2]	−97	−60	176	−176
Trp[3]	−62	−52	179	−176
Ala[4]	−62	−34	173	
Val[5]	−70	−51	176	−59
Gly[6]	−67	−41	179	
His[7]	−73	−44	−178	−174
Phe[8]	−93	−42	−172	−61
Leu[9]	−101			−58
peptide II				
Glp[1]		−137	174	47
Gln[2]	−47	−47	170	−173
Trp[3]	−64	−70	−171	−177
Ala[4]	−60	−35	+175	
Val[5]	−61	−66	+171	−58
Gly[6]	−69	−22	+174	
His[7]	−69	−39	−176	−176
Phe[8]	−103	+179		−64
Leu[9]	−96			−62

[a] Values are averages of the last 64 conformations from the dynamics trajectory (see text).

Table IV: Comparison of Experimental and Calculated Interproton Distances (Å) in the Backbone of Peptide II

atoms	exptl	calcd
peptide I		
Glp[1] HN–Gln[2] HN	2.8	2.9
Gln[2] HN–Trp[3] HN	2.8	2.8
Trp[3] HN–Ala[4] HN	2.6	3.0
Ala[4] HN–Val[5] HN	*a*	3.0
Val[5] HN–Gly[6] HN	2.8	2.8
Gly[6] HN–His[7] HN	2.9	2.9
His[7] HN–Phe[8] HN	*a*	2.8
Phe[8] HN–Leu[9] HN	2.3	2.5
Glp[1] HA–Gln[2] HN	3.3	3.0
Gln[2] HA–Trp[3] HN	3.3	3.7
Ala[4] HA–Val[5] HN	3.5	3.7
Val[5] HA–Gly[6] HN	3.5	3.7
His[7] HA–Phe[8] HN	4.5	3.7
peptide II		
Glp[1] HN–Gln[2] HN	3.8	4.3
Gln[2] HN–Trp[3] HN	3.5	3.4
Trp[3] HN–Ala[4] HN	3.2	3.2
Ala[4] HN–Val[5] HN	2.8	3.2
Val[5] HN–Gly[6] HN	3.4	3.3
Gly[6] HN–His[7] HN	3.2	3.2
His[7] HN–Phe[8] HN	2.8	2.8
Glp[1] HA–Gln[2] HN	3.3	3.3
Gln[2] HA–Trp[3] HN	3.3	3.8
Ala[4] HA–Val[5] HN	3.6	3.7
Val[5] HA–Gly[6] HN	2.9	3.3
His[7] HA–Phe[8] HN	3.5	3.7
Phe[8] HA–Leu[9] HA	2.9	2.8

[a] Severe overlap to the diagonal peaks.

the NOE between the Trp indole ring and the β-CH_2 protons of His.

A common feature between the two peptides is a clustering of hydrophobic side chains of Trp[3], Ala[4], His[7], and Phe[8] on one face of the peptide, rendering the peptides some amphipathic character. The most notable, and the most significant, difference between the two structures is in the carboxyl-terminal dipeptide region. In peptide I the side chains of Phe[8] and Leu[9] are directed in opposite orientations whereas in peptide II they are directed toward the same side of the peptide. The most distinguishing NOE in the carboxyl terminus of each peptide is the strong $NH^{i,i+1}$ NOE in peptide I and the strong $C_\alpha H^{i,i+1}$ NOE in peptide II, in both cases between Phe[8] and Leu[9]. The latter NOE, corresponding to an interproton separation of 2.9 Å, is absent in peptide I. Such a close approach of the sequential α protons in a peptide bond would require a cis peptide bond arrangement in a normal peptide bond. Thus it appears that the $\psi[CH_2S]$ substitution mimics a cis peptide bond geometry in peptide II. A reduced $C_\alpha H^{i,i+1}$ distance is also reported in the crystal structure of Boc-Alaψ-[CH_2S]Phe-OH (Zanotti et al., 1988).

The two peptides studied here are analogs of the carboxyl-terminal nonapeptide segment of bombesin. The conforma-

tions of bombesin have been investigated by several groups in different environments (Carver & Collins, 1990; Erne & Schwyzer, 1987). Erne and Schwyzer (1987) studied its conformation in a phospholipid bilayer membrane using FT-IR. Craver and Collins (1990) investigated bombesin conformation in a mixed solvent of trifluoroethanol and water by 2D NMR. Both groups have reported an α-helical conformation for bombesin in the carboxyl-terminal region. Thus the relaxed helical conformation of peptide I, formed by three connected turns, is generally consistent with the proposed structure of the carboxyl-terminal region of bombesin. The observed conformational similarities, between peptide I and peptide II, at the amino-terminal region are consistent with the reports that in bombesin-like peptides the amino-terminal residues are involved in receptor binding and the carboxyl-terminal residues in receptor activation.

In conclusion, we have determined the conformations of a Bn/GRP receptor agonist and an antagonist in the micelle-bound states by the combined application of 2D NMR and distance-restrained molecular dynamics simulations. The inability of restrained molecular dynamics for an exhaustive search of the conformation space, within the simulation period, is a limitation of the combination of techniques employed in this study. However, the excellent agreement between the calculated structures and the experimental data strongly suggests that the reported conformations accurately represent the predominant conformations of the peptides averaged over the time scale of proton chemical shifts. The similarities and differences in these conformations should prove useful as a rational foundation for the design of more selective and potent antagonists for the receptor function. This conclusion is based on the assumption that the micelle-bound conformations of these peptides are accurate representations of their receptor-bound conformations. Structure–activity studies involving the introduction of conformational constraints based on the NMR-derived conformations are in progress to test the validity of this assumption.

ACKNOWLEDGMENT

We gratefully acknowledge Kenneth Cornelius for amino acid analyses and Brian Regg for FAB/MS analyses of the peptides.

SUPPLEMENTARY MATERIAL AVAILABLE

Two tables listing upper-bound distance constraints for molecular dynamics simulations (2 pages). Ordering information is given on any current masthead page.

REFERENCES

Aguayo, S. M., King, T. E., Waldron, J. A., Sherritt, Kane, M. A., & Miller, Y. E. (1990) *J. Clin. Invest. 86*, 838–844.

Bothner-By, A. A., Stephens, R. L., Lee, J.-M., Warren, C. D., & Jeanloz, R. W. J. (1984) *J. Am. Chem. Soc. 106*, 811–813.

Brahms, S., & Brahms, J. (1980) *J. Mol. Biol. 138*, 149–178.

Brown, M. R., Rivier, J., & Vale, W. (1978) *Life Sci. 21*, 1729–1734.

Carver, J. A., & Collins, J. G. (1990) *Eur. J. Biochem. 187*, 645–650.

Corps, A. N., Rees, L. H., & Brown, K. D. (1985) *Biochem. J. 231*, 781–784.

Coy, D. H., Heinz-Erian, P., Jiany, N.-Y., Sasaki, Y., Taylor, J., Moreau, J.-P., Wolfrey, W. T., Gardner, J. D., & Jensen, R. T. (1988) *J. Biol. Chem. 263*, 5056–5060.

Cuttitta, F., Carney, D. N., Mulshine, J., Moody, T. W., Fedorko, J., Fischler, A., & Minna, J. D. (1985) *Nature (London) 316*, 823–826.

Davis, D. G., & Bax, A. (1985) *J. Am. Chem. Soc. 107*, 2820–2821.

Erne, D., & Schwyzer, R. (1987) *Biochemistry 26*, 6316–6319.

Erspamer, V. (1988) *Ann. N.Y. Acad. Sci. 547*, 3–9.

Fanger, B. O., Wade, A. C., & Cardin, A. D. (1991) *Regul. Pept. 32*, 241–251.

Ghatei, M. A., Jung, R. T., Stevenson, J. C., Hillyard, C. J., Adrian, T. C., Lee, Y. C., Christofides, N. D., Larson, D. L., Mashiter, K., MacIntyre, I., & Bloom, S. R. (1982) *J. Clin. Endocrinol. Metab. 54*, 980–985.

Heimbrook, D. C., Boyer, M. E., Garsky, V. M., Balishin, N. L., Kiefer, D. M., Cliff, A., & Rieman, M. W. (1988) *J. Biol. Chem. 263*, 7016–7019.

Heimbrook, D. C., Saari, W. S., Balishin, N. L., Friedman, A., Moore, K. S., Riemen, M. W., Kiefer, D. M., Rotberg, N. S., Wallen, J. W., & Oliff, A. (1989) *J. Biol. Chem. 264*, 11258–11262.

Jeener, J., Meier, B. H., Bachman, P., & Ernst, R. R. (1979) *J. Chem. Phys. 71*, 4546–4557.

Jensen, R. T., & Coy, D. H. (1991) *Trends Pharmacol. Sci. 12*, 13–18.

Jensen, R. T., Jones, S. W., Folkers, K., & Gardner, J. D. (1984) *Nature (London) 309*, 61–63.

Jensen, R. T., Coy, D. H., Saeed, Z. H., Heinz-Erian, P., Mantey, S., & Gardner, J. D. (1988) *Ann. N.Y. Acad. Sci. 547*, 138–149.

Kessler, H., Griesinger, C., Kersebaum, R., Wagner, K., & Ernst, R. R. (1987) *J. Am. Chem. Soc. 109*, 607–609.

Kumar, A., Wagner, G., Ernsr, R. R., & Wuthrich, K. (1981) *J. Am. Chem. Soc. 103*, 3654–3658.

Marion, D., & Wuthrich, K. (1983) *Biochem. Biophys. Res. Commun. 113*, 967–974.

Marion, D., & Bax, A. (1989) *J. Magn. Reson. 83*, 205–211.

McDonald, T. J., Nelsson, G., Vagne, M., Ghatei, M., Bloom, S. R., & Mutt, V. (1978) *Gut 19*, 767–774.

Negri, L. (1986) *Eur. J. Pharmacol. 32*, 207–212.

Rivier, J. E., & Brown, M. R. (1978) *Biochemistry 17*, 1766–1771.

Saeed, Z. A., Huang, S. C., Coy, D. H., Jiang, N. Y., Heinz-Erian, P., Mantey, S., Gardner, J. D., & Jensen, R. T. (1989) *Peptides 10*, 597–603.

Schwyzer, R., & Erne, D. (1987) *Biochemistry 26*, 6316–6319.

Spatola, A. F., & Edwards, J. V. (1986) *Biopolymers 25*, S229–S244.

Spindel, E. R., Giladi, E., Brehm, P., Goodman, R. H., & Segerson, T. P. (1990) *Mol. Endocrinol. 4*, 1956–1963.

States, D. J., Haberkorn, R. A., & Reuben, D. J. (1982) *J. Magn. Reson. 48*, 286–292.

Sunday, M. E., Hua, J., Dai, H. B., Nusrat, A., & Torday, J. S. (1990) *Am. J. Respir. Cell. Mol. Biol. 3*, 199–205.

Van Tol, E. A. F., Elzo Kraemer, C. V., Verspaget, H. W., Masclee, A. M., & Lamers, C. B. H. W. (1991) *Neuropeptides 18*, 15–21.

Wharton, J., Polak, J. M., Bloom, S. R., Ghetei, M. A., Solcia, E., Brown, M. R., & Pearsi, A. G. E. (1978) *Nature (London) 273*, 769–770.

Zanotti, B. G., Toniolo, C., Owen, T. J., & Spatola, A. F. (1988) *Acta Crystallogr. C44*, 1576–1579.